Available online at www.sciencedirect.com

ScienceDirect

Procedia Structural Integrity 57 (2024) 404–410

Structural Integrity Procedia

www.elsevier.com/locate/procedia

Fatigue Design 2023 (FatDes 2023)

Analysis of the uniaxial fatigue behaviour of 42CrMo4 Q&T steel specimens extracted from the big end of a marine engine connecting rod using the heat dissipation approach

Sofia Pelizzoni[a], Mauro Ricotta[a], Alberto Campagnolo[a], Giovanni Meneghetti[a]*

[a]*Department of Industrial Engineering, University of Padova, Via Venezia 1, Padova 35131, Italy*

Abstract

Among the energy-based approaches to estimate the fatigue life of steel specimens, the experimental method based on the heat dissipation (or intrinsic dissipation) per cycle, Q, proved effective for correlating the effects of geometrical stress concentrations, uniaxial and multiaxial loadings, and mean stress. The mean stress effect requires a properly defined temperature-corrected parameter $\bar{Q}$. The parameter Q is readily evaluable using temperature measurements and in this investigation it has been employed for fatigue strength assessment of plain specimens, extracted from a 42CrMo4 Q&T connecting rod big end of a marine engine. Completely reversed, strain-controlled, constant amplitude fatigue tests were carried out and the Q parameter evolution was monitored during each test by suddenly stopping the fatigue test several times and measuring the cooling gradient of material temperature. As result, besides the traditional strain-life (ε_a-$2N_f$) curve, the Q-N_f curve was also obtained, which is expected to be applicable for correlating notch and mean stress effects in future investigations.

Keywords: fatigue, connecting rod, 42CrMo4 Q&T, energy methods, specific heat loss

* Corresponding author. Tel.: +39 049 827 67 51
E-mail address: giovanni.meneghetti@unipd.it

10.1016/j.prostr.2024.03.043

1. Introduction

The heat dissipation (or intrinsic dissipation) per cycle, Q, has been proposed as fatigue damage index in (Meneghetti 2007) along with the experimental procedure for its evaluation, which is based on the measurement of the material temperature undergoing fatigue. More precisely, the experimental evaluation of Q is based on the cooling gradient of the material which is measured immediately after a sudden stop of the fatigue test (time t^* in Figure 1). Before test stopping, the material temperature must be stationary, i.e. the heat dissipation per cycle equates the heat transfer to the environment by conduction, convection and radiation, as shown in Figure 1. The Q parameter can be calculated according to Eq. (1):

$$Q = \frac{\rho \cdot c \cdot \left.\frac{\partial T}{\partial t}\right|_{t=(t^*)^+}}{f_L} \tag{1}$$

where ρ is the material density, c is the material specific heat and f_L is the load test frequency and T(t) is the time-variant material temperature and t* is the time when the fatigue test has been suddenly interrupted.

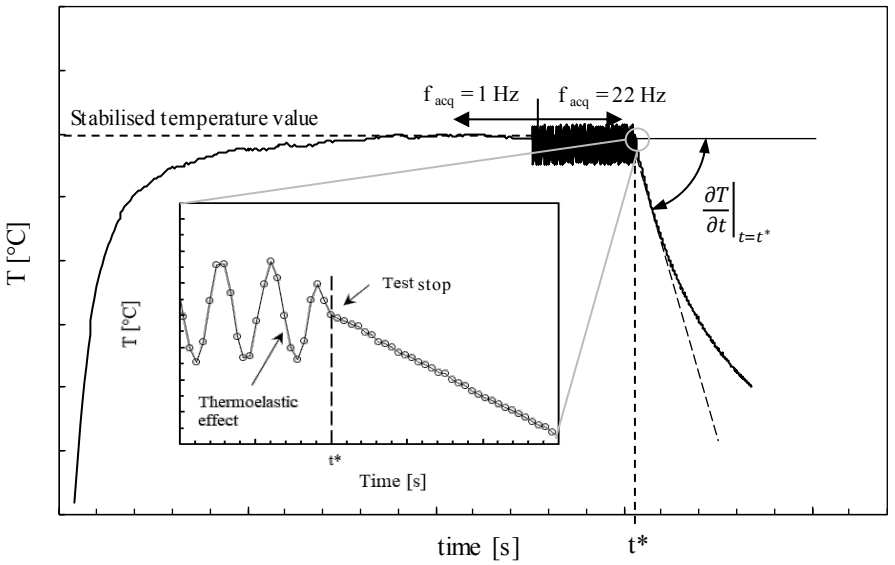

Figure 1. Experimental evaluation of the heat dissipation per cycle by measuring the cooling rate at t = t*. Temperature oscillations for t < t* due to the thermoelastic effect are shown in the detailed view.

The Q parameter was initially adopted to correlate in a single scatter band more than 140 experimental results generated from constant-amplitude, fully reversed, stress- or strain- controlled fatigue tests on AISI 304L hot-rolled plain or notched specimens (notch radii between 0.5 and 8 mm) (Meneghetti and Ricotta 2012; Rigon et al. 2017a) and from cold drawn unnotched bars of the same steel under zero-mean stress axial or torsional fatigue loadings (Meneghetti et al. 2013), as shown in Figure 2a. Subsequently, the Q-based approach was extended to analyse the influence of the mean stress, which required to combine the Q-parameter with the thermoelastic temperature related to the maximum stress of the load cycle (Meneghetti et al. 2016) and resulted in a temperature-corrected energy parameter $\bar{Q}$. The proposed approach was applied to collapse into a single scatter band fatigue data obtained on cold drawn AISI 304L stainless steel (see Figure 2b) and hot rolled quenched and tempered C45 steel specimens tested at different load ratios. In a recent investigation (Rigon et al. 2021), the energy approach has been adopted to successfully correlate fatigue test data generated from specimens made of C45 steel and subjected to in-phase and out-of-phase axial/torsional multiaxial fatigue loadings.

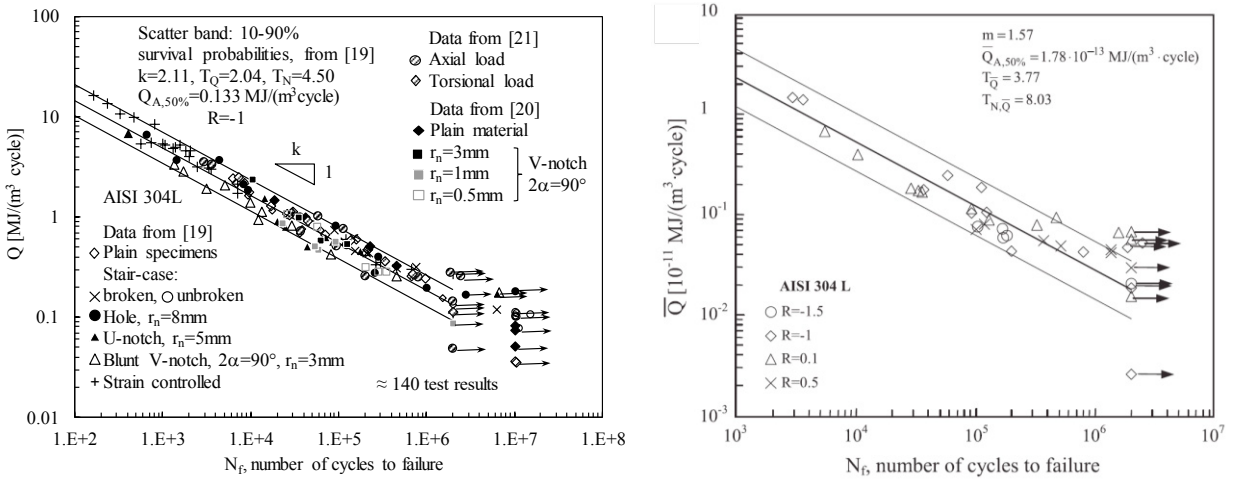

Figure 2. Fatigue data generated from specimens made of AISI 304L steel analysed in terms of (a) heat dissipation per cycle Q to account for specimen geometry and loading conditions (Rigon et al. 2017b); (b) the temperature-corrected energy parameter $\bar{Q}$ to account for mean stress effect (Meneghetti et al. 2016). Used with permission of Elsevier, from (Rigon et al. 2017b) and (Meneghetti et al. 2016), respectively, permission conveyed through Copyright Clearance Center, Inc.

Among the energy-based fatigue indexes, the hysteresis energy per cycle, W, proposed by Ellyin (Ellyin 1996) and the total mechanical energy expended to failure proposed by Halford (Halford 1966) are worth mentioning.

2. Material, specimen geometry and test methods

The aim of the present work is to investigate the fatigue strength of a 42CrMo4 Q&T connecting rod big end of a marine engine by adopting the Q-based approach. Accordingly, specimens were extracted from the big end of a connecting rod along radial directions, to account for the effects of the manufacturing processes. The main physical properties and the chemical composition of the material are reported in Table 1, while the geometry of the connecting rod big end has not been reported for confidentiality reasons.

Table 1. Material properties, Ramberg-Osgood parameters (Eq. (2)) and chemical composition of 42CrMo4 steel

ρ [kg/m³]	*c* [J/(kg K)]	E_s [MPa]	$\sigma_{p0.2}$ [MPa]	σ_R [MPa]	A [%]	K [MPa]	n [/]	C [%]	Mn [%]	Si [%]	Cr [%]	Ni [%]	Mo [%]	Cu [%]
7850	460	214500	656	860	8.68	993	0.0669	0.397	0.840	0.330	1.10	0.26	0.25	0.21

A MTS 858 MiniBionix II axial servo-hydraulic testing machine with 15 kN load capacity and a MTS TestStar IIm digital controller, has been employed to perform both static tensile tests and strain-controlled fatigue tests at room temperature. The axial strain has been measured with an extensometer MTS 632.13F-20 having gauge length of 10 mm.

Static tensile tests have been carried out on three plain cylindrical specimens (Figure 3a) under displacement control according to ASTM E8 (2016) and by imposing a displacement rate of 0.375 mm/min. After each test, the static Young's modulus E_s, the engineering proof stress $\sigma_{p,0.2}$, the engineering tensile strength σ_R and the elongation after fracture A% have been derived and the average values are reported in Table 1.

Strain-controlled fatigue tests have been carried out on plain cylindrical specimens (Figure 3b) according to ASTM E 606-04 (2004) by imposing a sinusoidal wave form with a nominal strain ratio $R_\varepsilon = -1$ and run-out condition at $2 \cdot 10^6$ cycles. Before performing the fatigue tests, the residual stress component along the specimen longitudinal axis has been measured for each specimen by adopting a SpiderX™ GNR diffractometer and resulted equal to σ_{res} = -559 ± 83 MPa. To mitigate residual stresses, a surface layer of approximately 50 μm has been removed from each specimen by polishing (electrolytic machine Struers™ Lectropol 5). After polishing, the longitudinal residual stress component

was reduced by a considerable amount and resulted σ_{res} = -139 ± 36 MPa. The adopted test frequencies f_L have been in the range between 0.3 and 6 Hz, depending on the applied strain amplitude. The signals from the load cell and the extensometer have been cross-plotted to derive the hysteresis loops, where stabilization has been assumed at half the fatigue life according to ASTM E 606-04 (2004). The temperature has been monitored during all fatigue tests by means of a copper–constantan thermocouple having accuracy 0.02 °C and fixed at the gauge section of the specimens by means of a silver-loaded conductive epoxy glue. A data logger Agilent Technologies HP 34970A operating at a sample frequency of f_{acq} = 22 Hz has been adopted to acquire the temperature signals measured by the thermocouples. To monitor the evolution of Q during each test, 1 to 8 cooling gradients (depending on the applied strain level) were performed by following the procedure proposed in (Meneghetti 2007).

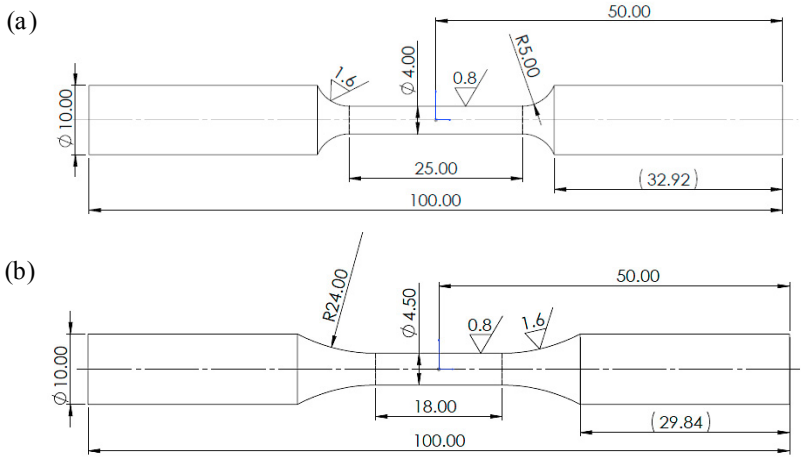

Figure 3. Geometry of the plain specimens adopted for (a) the static tensile tests and (b) the strain-controlled fatigue tests.

3. Results of experimental tests

Figure 4 reports the monotonic static tensile curve and the fitted parameters according to the Ramberg-Osgood expression (Eq. (2)).

$$\varepsilon = \frac{\sigma}{E_s} + \left(\frac{\sigma}{K}\right)^{\frac{1}{n}} \tag{2}$$

where K and n are the strength coefficient and the strain hardening exponent, respectively. It is worth mentioning that K and n reported in Table 1 and inside Fig. 4 have been fitted on the engineering stress-strain data up to a strain value equal to 0.8%.

Figure 4 reports the half-life hysteresis loops along with the cyclic stress-strain curve, which has been determined by fitting the tips of the hysteresis loops for different applied strain amplitudes adopting a Ramberg-Osgood-type expression (Eq. (2)). The resulting K' and n' parameters are reported inside the figure. Comparing the monotonic and the cyclic stress-strain curves, it is concluded that the 42CrMo4 Q&T steel exhibits a softening behavior.

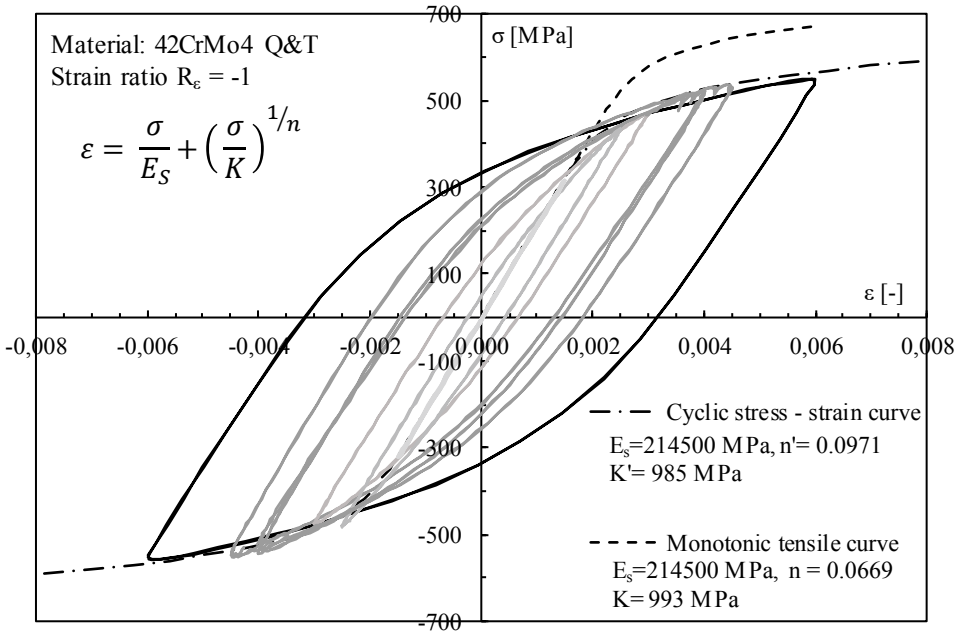

Figure 4. Half-life hysteresis loops, monotonic and cyclic curves.

The experimental results ε_a versus $2N_f$ are presented in Figure 5 and they have been fitted using the Basquin (Basquin 1910), Manson (Manson 1954), and Coffin (Coffin 1954) equations, i.e. by dividing the total strain amplitude ε_a into its elastic ($\varepsilon_{a,el}$) and plastic ($\varepsilon_{a,pl}$) components (Eq. 3), the fitted parameters being reported in Fig. 5.

$$\varepsilon_a = \varepsilon_{a,el} + \varepsilon_{a,pl} = \frac{\sigma_f'}{E}\left(2 \cdot N_f\right)^b + \varepsilon_f'\left(2 \cdot N_f\right)^c \tag{3}$$

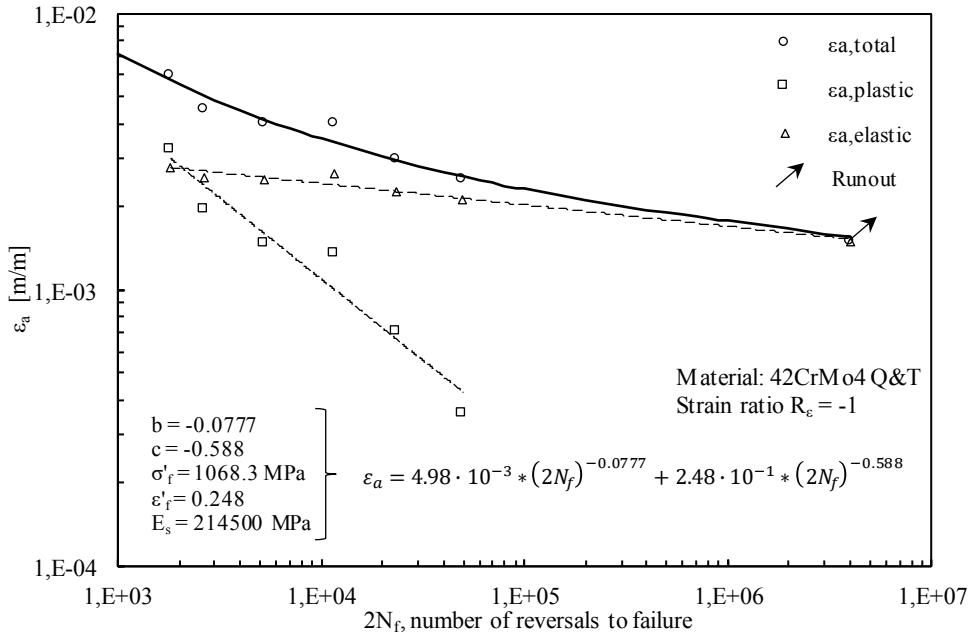

Figure 5. Strain-controlled fatigue test results and parameters of the Manson-Coffin curve fitted on experimental data.

The temperature at the specimen's surface increased in the range 6–21 °C from the beginning of the fatigue test, depending on the applied strain amplitude and the adopted loading frequency. Figure 6 shows the temperature data measured during the cooling phase for two exemplary specimens. After evaluating the cooling gradient, Q was calculated by means of Eq. (1) with the material parameters of Table 1 and the relevant loading frequency f_L.

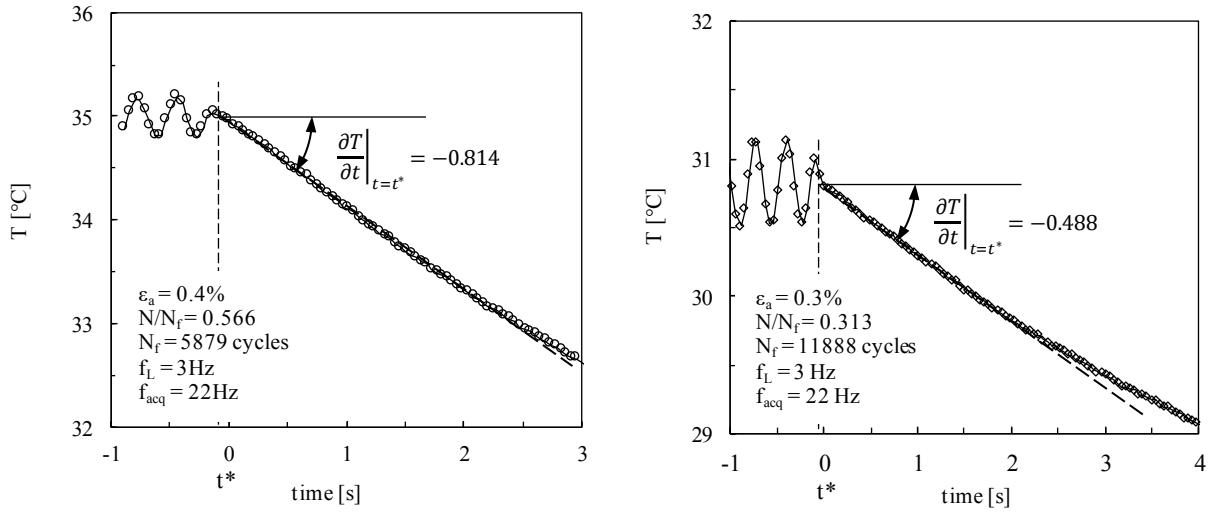

Figure 6. Experimental evaluation of the specific heat loss during two strain-controlled fatigue tests on plain specimens.

Taking Q calculated at 50% of the total fatigue life of individual specimens, Figure 7a shows the energy-based fatigue curves, the resulting scatter band referred to a survival probability of 10% and 90% with a confidence level of 95%, the inverse slope k, the mean energy value $Q_{A,50\%}$ referred to $N_A = 2 \cdot 10^6$ cycles, the energy-based scatter index T_Q and the life-based scatter index $T_{N,Q}$.

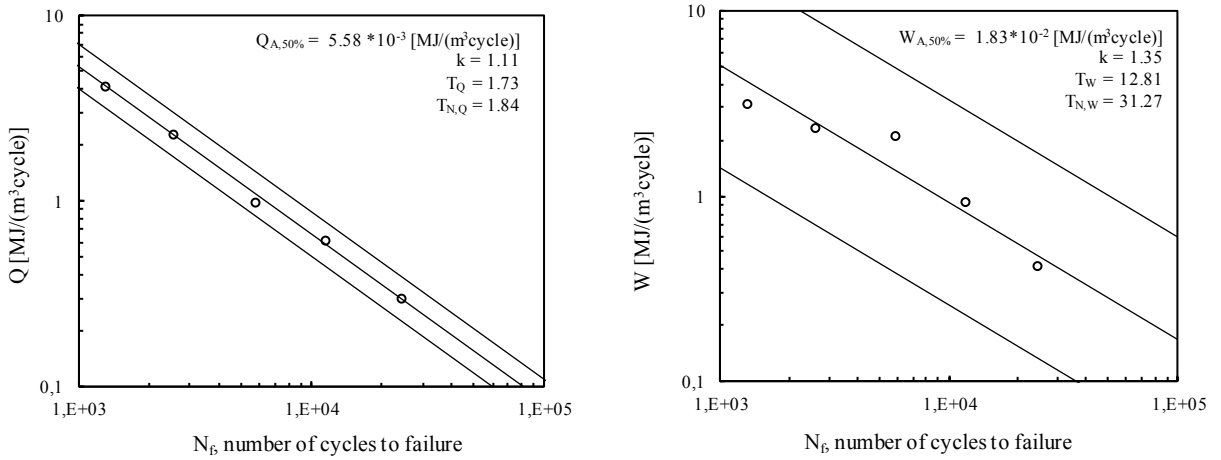

Figure 7. Fatigue test results on the plain specimens made of 42CrMo4 Q&T steel in terms of (a) heat dissipation per cycle Q, and (b) plastic strain hysteresis energy W.

The same experimental data reported in Fig. 7a have been re-analysed in terms of the plastic strain hysteresis energy W and are reported in Figure 7b. By comparing Fig. 7a with Fig. 7b, the scatter index of the Q-based synthesis is significantly lower than that derived when using W. Fig. 7 reports the Q- and W-based fatigue curves using a constant slope in logarithmic scales from the low to the medium cycle fatigue regimes, according to (Ellyin 1996). The Q-

based fatigue curve reported in Figure 7a can be used for correlating notch effects in fatigue tests of specimens and components.

4. Conclusions

Static and push–pull, strain-controlled fatigue tests have been performed on plain specimens, extracted from a 42CrMo4 Q&T steel big end of connecting rod of a marine engine. The monotonic and cyclic stress-strain curves as well as the strain-life (ε_a-$2N_f$) curve have been determined and afterwards the experimental data have been re-analysed by adopting the heat dissipation per cycle Q and a scatter band has been fitted on available data. The scatter index of the Q-based synthesis was seen to be significantly lower than that derived when using the plastic strain hysteresis energy W. The use of the heat dissipation per cycle appears convenient in practical applications since it is readily valuable using temperature measurements. On the basis of previous works focused on different steel grades, the Q-based scatter band calibrated in the present work is expected to correlate notch and mean stress effects, the latter requiring an existing temperature-corrected parameter $\bar{Q}$.

Acknowledgements

This work was co-funded by the European Union (Grant Agreement No. 101058179; ENGINE). However, the views and opinions expressed are those of only the authors and do not necessarily reflect those of the European Union or the European 380 Health and Digital Executive Agency. Neither the European Union nor the granting authority can be held responsible for these opinions.

References

Basquin OH (1910) The exponential law of endurance tests. Am Soc Test Mater Proc 10:625–630

Coffin LF (1954) A study of the effect of cyclic thermal stresses on a ductile metal. Trans ASME 76:931–950

Ellyin F (1996) Fatigue Damage, Crack Growth and Life Prediction. Springer Netherlands, Dordrecht

Halford GR (1966) The energy required for fatigue. J Mater 19:3–18

Manson SS (1954) Behavior of materials under conditions of thermal stress. Report No. NACA TN-2933

Meneghetti G (2007) Analysis of the fatigue strength of a stainless steel based on the energy dissipation. Int J Fatigue 29:81–94. https://doi.org/10.1016/j.ijfatigue.2006.02.043

Meneghetti G, Ricotta M (2012) The use of the specific heat loss to analyse the low- and high-cycle fatigue behaviour of plain and notched specimens made of a stainless steel. Eng Fract Mech 81:2–16. https://doi.org/10.1016/j.engfracmech.2011.06.010

Meneghetti G, Ricotta M, Atzori B (2016) A two-parameter, heat energy-based approach to analyse the mean stress influence on axial fatigue behaviour of plain steel specimens. Int J Fatigue 82:60–70. https://doi.org/10.1016/j.ijfatigue.2015.07.028

Meneghetti G, Ricotta M, Negrisolo L, Atzori B (2013) A Synthesis of the Fatigue Behavior of Stainless Steel Bars under Fully Reversed Axial or Torsion Loading by Using the Specific Heat Loss. Key Eng Mater 577–578:453–456. https://doi.org/10.4028/www.scientific.net/KEM.577-578.453

Rigon D, Berto F, Meneghetti G (2021) Estimating the multiaxial fatigue behaviour of C45 steel specimens by using the energy dissipation. Int J Fatigue 151:106381. https://doi.org/10.1016/j.ijfatigue.2021.106381

Rigon D, Ricotta M, Meneghetti G (2017a) An analysis of the specific heat loss at the tip of severely notched stainless steel specimens to correlate the fatigue strength. Theor Appl Fract Mech 92:240–251. https://doi.org/10.1016/j.tafmec.2017.09.003

Rigon D, Ricotta M, Meneghetti G (2017b) An analysis of the specific heat loss at the tip of severely notched stainless steel specimens to correlate the fatigue strength. Theor Appl Fract Mech 92:240–251. https://doi.org/10.1016/J.TAFMEC.2017.09.003

(2016) ASTM E8/E8M-16 - Standard Test Methods for Tension Testing of Metallic Materials

(2004) ASTM E 606-04 - Standard practice for Strain-Controlled fatigue testing. ASTM International